ARTICLE

Animal Models

Human adipose tissue mesenchymal stem cells as a novel treatment modality for correcting obesity induced metabolic dysregulation

Nitya Shree[1] · Sunil Venkategowda[2] · M. V. Venkatranganna[3] · Indrani Datta[4] · Ramesh R. Bhonde[1,5]

Abstract

Objective Obesity induced metabolic dysregulation results in cluster of chronic conditions mainly hyperglycemia, hyper-insulinemia, dyslipidemia, diabetes, cardiovascular complications and insulin resistance. To investigate the effect of *i.m.* injection of human adipose tissue derived mesenchymal stem cells and its secretome in correcting obesity induced metabolic dysregulation in high fat diet fed obese model of mice and understand its mechanism of action.

Subjects We injected human adipose tissue derived mesenchymal stem cells (ADMSCs) suspension (CS), conditioned medium (CM) and the cell lysate (CL) intramuscularly in high fat diet (HFD)-induced C57BL/6 mice. Metformin was used as a positive control. ADMSCs were traced in vivo for its bio distribution after injection at different time points.

Results ADMSCs-treated mice exhibited remarkable decrease in insulin resistance as quantified by HOMA-IR and trigly-ceride glucose index with concomitant decrease in oxidized LDL and IL6 as compared with the untreated control. CS injection showed improvement in glucose tolerance and reduction in fatty infiltration in the liver, macrophage infiltration in adipose and hypertrophy of the islets resulting from HFD. Upregulation of miRNA-206, MyoD and increase in protein content of the skeletal muscle in CS-treated mice indicates plausible mechanism of action of ADMSCs treatment in ameliorating IR in HFD mice.

Conclusion Of all the three treatments, CS was found to be the best. ADMSCs were found to have migrated to different organs in order to bring about the correction in dysregulated metabolism induced by obesity. Our results open up a novel treatment modality for possible therapeutic usage in human subjects by employing autologous or allogeneic ADMSCs for the better management of obesity induced metabolic dysregulation.

Introduction

Obesity induced metabolic dysregulation results in cluster of chronic conditions mainly hyperglycemia, hyperinsulinemia, dyslipidemia, diabetes, cardiovascular complications, and insulin resistance [1]. Metabolic pathways in our body have developed to deliver energy to tissues in times of physical threat and survival, or to efficiently save energy in times of food deprivation. Today, the combination of abundance of food and lack of physical activity has led to excessive nutrient storage, introducing major stress on our metabolic pathways, resulting in an increase in the occurrence of disease originating from metabolic dysfunction [2].

Stem cells have a great potential for basic research and also hold the future for clinical applications. The characteristic features of these cells are quite unique from somatic cells [3]. The area of mesenchymal stem cell (MSC) research has bloomed recently. MSCs are known to be multipotent and have the ability of self-renewal and differentiation into several mesodermal cell lineages and certainly have the capacity to repair several damaged tissues [4, 5].

Adipose-derived mesenchymal stem cells (ADMSCs) are emerging as a source of stem cells that can be obtained by a

✉ Ramesh R. Bhonde
rrbhonde@gmail.com

1 School of Regenerative Medicine, Manipal Academy of Higher Education, Bangalore, India

2 Department of Biotechnology, Jain University, Bangalore, India

3 Connexios Life Sciences Pvt. Ltd., Bangalore, India

4 Department of Biophysics, NIMHANS, Bangalore, India

5 Dr. D.Y. Patil Vidyapeeth, Pune, India

less invasive method and in larger quantities than from BM. These cells can be isolated from human lipoaspirates and, like MSCs, can differentiate toward osteogenic, adipogenic, myogenic, chondrogenic, and especially neurogenic lineages 3. ADMSCs, can be readily isolated from fat tissue after liposuction and easily expanded in culture in large numbers, have developed an striking source for cell therapy [6, 7]. Si et al. demonstrated a novel role of MSC administration in improving insulin sensitivity and showed improved GLUT4 expression and the member translocation in peripheral insulin target tissue through an insulin independent manner [8]. It has been reported earlier that systemic transplantation of MSC ameliorates HFD-induced obesity and restores metabolic balance through multisystemic regulations that are niche dependent [9]. Multiple infusions of MSCs promote prolonged decrease in hyperglycemia and apoptosis in pancreatic islets and increases insulin sensitivity in HFD fed mice [10].

We have shown earlier the role of subcutaneous injection of ADMSCs and its CM in reversing acute inflammatory condition in vivo [11]. We have also demonstrated the role of ADMSCs CM in improvement of insulin resistant state in vitro [12]. Nonetheless, we were interested in investigating the role of ADMSCs in obesity induced metabolic dysregulation in vivo. Therefore, based on previous findings, we hypothesized that multiple *i.m.* injections of ADMSCs may help in normalizing the dysregulated metabolism of diet induced obese (DIO) animals. Here, we demonstrate for the first time the importance of human ADMSCs therapy in improving obesity induced metabolic dysregulation in DIO mice by migrating to different organs.

Methods

Study design

DIO model of mice was developed by feeding the mice on HFD [13]. Six-week-old male C57BL/6 mice were procured from Vivo biosciences, Hyderabad, India. Animals were housed in polypropylene cages, maintained at $23 \pm 1\,^{\circ}$C, $60 \pm 10\%$ humidity, exposed to 12 h cycles of light and dark and had access to diet and water ad libitum throughout the experimental period. After acclimatization for a week, mice were fed either on chow diet (10% Kcal, Research Diet Inc., NJ, D10001) or High fat diet (HFD) (60% kcal from fat; Research Diet Inc., NJ, USA - D12492) for 10 weeks. Animal experiment protocols and experimental procedures were approved by the Connexios Institutional Animal Ethics Committee which are in agreement with the ARRIVE guidelines [14, 15]. Mice were grouped ($n = 6$) based on their body weight and oral glucose tolerance test (OGTT).

Animals were grouped for treatment and intramuscular injection (in Rectus Femoris muscle) of ADMSCs suspension (CS), 50% of the conditioned media (CM) and the cell lysate (CL) was given in 0.1 ml volume, twice at an interval of 4 weeks. Metformin was used as a positive control (300 mg per kg body weight, orally, daily). A total of 0.1 ml of the culture media was injected in the untreated group (vehicle control).

ADMSCs preparation

ADMSCs were procured from ANSA, Bangalore, India. ADMSCs were cultured in DMEM with high glucose, 10% fetal bovine serum and characterized by Flow cytometry using CD 105, CD90, CD34, and HLA-DR markers. ADMSCs were confirmed for the mesenchymal characteristics by their trilineage differentiation potential *viz.* adipogenesis, osteogenesis and chondrogenesis. For the treatment, cells were trypsinized, 5×10^5 cells were resuspended in 0.1 ml of the growth media and injected per animal through *i.m.* route.

Preparation of CM

ADMSCs were grown as mentioned above. Once the cells attained 90–100% confluency, CM was collected, filtered and diluted 50% with the growth media. 0.1 ml was injected per animal intramuscularly.

Preparation of the cell lysate

For the preparation of cell lysate, 5×10^5 cells were resuspended in 0.1 ml of the growth media, sonicated and spun down at 1400 rpm for 5 min. The supernatant was used for the treatment (0.1 ml).

Glucose measurements

Animals were kept on fasting for 6 h and blood was collected from tail vein for the measurement of fasting glucose using Accu- Chek Active glucometer (Roche Diagnostics) every week till the end of the study.

Triglyceride estimation

At the end of the study, animals were fasted overnight and triglyceride was measured using the Accutrend Plus system (Cobas, Roche, Mannheim, Germany).

Oral glucose tolerance test (OGTT)

Oral glucose load of 2 g per kg body weight was given with an oral gavage and OGTT was determined as demonstrated

by Wang et al. [13]. Glucose was measured at different time points viz. 0, 30, 60, 120 min using an Accu-Chek Active glucometer (Roche, Mannheim, Germany) by collecting the blood from the tail vein.

Measurement of insulin

Animals were fasted for 6 h and blood sample was collected by retro orbital puncture. Serum insulin was measured using Ultra sensitive mouse Insulin ELISA kit from Crystal chem, Downers Grove, USA.

Serum oxidized low density lipoprotein ELISA

Blood was collected by retro orbital puncture from the animals fasted overnight. Serum samples were evaluated for oxidized LDL using ELISA kit from Mercodia AB, Uppsala, Sweden. All the procedure were performed as per the manufacturer's instructions.

Serum interleukin-6 ELISA

Serum samples were assayed for IL6 using the Quantikine ELISA kit from R&D systems Inc. Minneapolis, USA following the instructions provided in the user manual.

Assessment of insulin resistance

Homeostatic model assessment of insulin resistance (HOMA-IR) was calculated by using the formula (Fasting insulin (mg/dL) × Fasting glucose (mg/dL)/405 to assess the state of Insulin resistance. Triglyceride glucose index (TyG) was calculated using (TG (mg/dL) × glucose (mg/dL)/2).

Histopathological studies

Liver, muscle, subcutaneous adipose and pancreatic tissues were fixed in formalin and 4 μm sections were stained with hematoxylin and eosin (H&E) stain. Picrosirius red staining was performed for the muscle sections. The images were captured using an inverted microscope (Nikon Eclipse TE2000-5, Japan).

Hepatic triglyceride estimation

Liver tissue triglyceride was estimated by the Folch's method. Briefly, lipids were extracted with chloroform: methanol (2:1) mixture, the organic layer was separated and dried. The residue was resuspended in 0.1 ml of isopropyl alcohol, and triglycerides was quantified using Triglyceride quantification kit (Diagnostic systems, Germany).

Gene expression analysis

Tissues collected in trizol were lysed using the bead lyser from Qiagen. RNA was extracted, cDNA conversion was carried out using High-Capacity cDNA Reverse Transcription Kit from Applied Biosystems. RT-PCR was performed using Kappa Sybr green. Relative gene expression pattern was analyzed. Data represented as the fold of expression.

miRNA-206 analysis

Micro RNA (miRNA) from muscle tissue was isolated using miRNeasy Mini Kit from Qiagen, Hilden, Germany. After quantifying the miRNA, cDNA conversion was carried out using TaqMan® MicroRNA Reverse Transcription Kit from Applied Biosystems, Vilnius, Lithuania.miRNA-206 gene expression was performed by using TaqMan® Universal Master Mix II from Applied Biosystems, Foster City, CA, USA. Relative gene expression was calculated by normalizing to the U6 snRNA levels.

Protein quantification

Mice were sacrificed by cervical dislocation at the end of the study. One hundered micrograms of the muscle tissue was collected in the protein lysis buffer containing protease and phosphatase inhibitors. Protein quantification was carried out by the Bradford assay using Bio-rad Protein assay reagent from Biorad Laboratories, Inc. USA. Total protein content in the skeletal muscle is represented as microgram of protein per milligram of tissue (μg of protein/mg of tissue).

LCMS/MS

Two micrograms of protein was loaded on column for IDA run using Triple TOF 5600+ AbSciex. Peak view software (AbSciex) was used to visualize the chromatogram and Protein pilot software (AbSciex) was used to obtain the protein identity.

In vivo tracking of the cells

To track the ADMSCs after transplantation, the cells were labeled using the CellVue™ NIR815 Cell Labeling Kit before injection and the whole animal noninvasive imaging in NIR range was performed at day 0, week 4, and week 8, respectively. Another set of mice were dissected to perform organ imaging at these time points to understand the biodistribution of the cells. ADMSCs were injected in the right thigh muscle and by using the Li-COR Pearl Impulse software version 2.0 image analysis tools, regions of interest was identified and normalized fluorescence (total relative

fluorescence/total area) of the right and left thigh muscle were represented.

Statistical analysis

All data presented are mean ± SEM. Groups were compared using one way ANOVA (Bonferroni's Multiple Comparison Test using GraphPad Prism software) and Student's t test. P value ≤ 0.05 were considered as statistically significant. HOMA-IR index was calculated using the predefined formula for calculating the levels insulin resistance. TyG was also calculated as described earlier.

Results

Health status of the mice

All the mice were healthy pathogen free before the starting the experiment (Data available on request).

DIO model development

A twofold significant increase in the body weight of the DIO mice was observed as compared with the lean control. Mice were allocated into six different groups for treatment based on the body weight and OGTT of the mice (Supplementary Fig. 1A). There was a ~2-fold increase in the body weight of the HFD mice as compared with the LC (Supplementary Fig. 1B, C). Serum triglyceride was significantly high compared with the lean control (Supplementary Fig. 2A). Glucose tolerance was impaired in the mice fed with HFD for 10 weeks (Supplementary Fig. 2B, C).

Characterization of ADMSCs

ADMSCs were characterized for the MSC markers by flow cytometry analysis. ADMSCs were positive for CD 105 and CD 90. Markers negative for ADMSCs were HLA DR and CD 34 (Supplementary Fig. 3A). The ability of the ADMSCs to differentiate into trilineage viz. osteocytes, chondrocytes, and adipocyte was confirmed by differentiation and staining of the cells. Oil O red staining showed adipogenic differentiation, Alizarin Red staining for Osteogenic differentiation and Alcian blue staining for chondrogenesis. (Supplementary Fig. 3B).

Effect of the treatment on body weight

At the end of 8th week of treatment, metformin showed twofold decrease in the body weight and there was no significant change in any of the other treatments as compared with the HFD control. (Supplementary Fig. 4)

Restoration of the normoglycemic status

There was no significant change observed during the initial weeks of the treatment (Fig. 1a). At the end of 8th week of the treatment; there was a significant decrease in the fasting glucose levels (Fig. 1b) The positive control metformin showed substantial decrease compared with the HFD control ($p < 0.001$). Treatment with CS, CM, and CL also exhibited significant glucose lowering capacity CS ($p < 0.01$), CM ($p < 0.05$), and CL ($p < 0.05$).

Improvement in the glucose tolerance

As stated earlier, OGTT represents the most physiological route of entry of glucose [15]. Glucose tolerance after an oral dose of 2 g/kg body weight of glucose improved in metformin ($p < 0.01$) as well as CS-treated group ($p < 0.05$) as shown in Fig. 1c. Area under curve (AUC) is inversely proportional to the tolerance derived using GraphPad prism software as depicted in Fig. 1d.

Reduction in triglyceridemia

At the end of the study, all the treatment groups showed significant decrease in serum triglyceride levels which was comparable to the positive control metformin. All the treatment groups shared the same p value of <0.01 (Fig. 1e, f).

Effect of treatment on hyperinsulinemia

One of the features of the IR is hyperinsulinemic condition. Mice fed on HFD attained hyperinsulinemia as compared with the lean control ($p < 0.001$). On the other hand, all the treatment groups showed significant reduction in the serum insulin levels except for the CL-treated group (Fig. 2a).

Cytokine analysis

We investigated the status of proinflammatory cytokine namely IL6 and found a dramatic reduction in the secreted IL6 by CS ($p < 0.05$) and CM ($p < 0.05$). Metformin and CL did not show any significant change as shown in Fig. 2b. Figure 2c depicts the reduction in oxidized LDL which also showed substantial decrease in all the treatment groups ($p < 0.05$).

Hepatic triglyceride analysis

Hepatic triglyceride levels were high in the HFD control than lean control ($p < 0.05$). CS reduced liver triglycerides significantly as compared with HFD control ($p < 0.01$) (Fig. 2d).
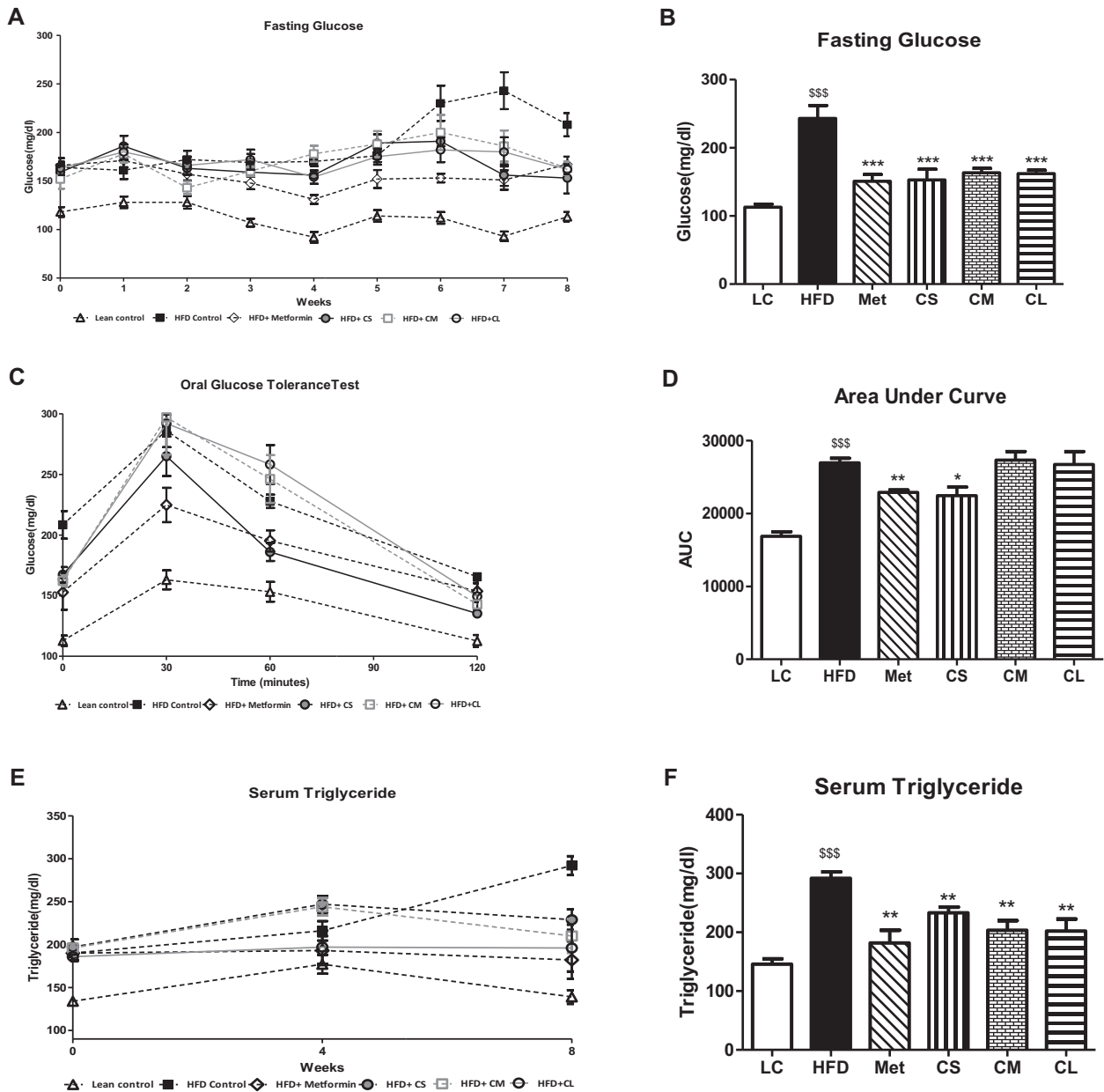
Fig. 1 Restoration of normoglycemia correlated with reduction in triglyceride levels and improvement of glucose tolerance: (**a**) Fasting glucose levels of the mice from week 0 to week 8 of the treatment. (**b**) Fasting glucose levels at the end of week 8. (**c**) Serum triglyceride levels at four weeks interval (**d**) Serum triglyceride levels at the end of the study (Week8). (**e**) OGTT at different time intervals (0, 30, 60 and 120 min). (**f**) OGTT confirmed by Area Under the Curve (AUC), derived using GraphPad Prism software version5.0. All data presented are mean ± SEM. Significance levels '$' shows HFD compared with LC and '*' shows comparison with untreated HFD control

Assessment of insulin resistance

In accordance with the earlier reports which states that HOMA IR and TyG are the useful and reliable indicators of Insulin resistance, our data shows a remarkable decrease in HOMA IR (Fig. 2e) and TyG (Fig. 2f) in all the treatment groups as compared with HFD control.

Impact on tissue architecture

In an attempt to understand the tissue architecture of the untreated and the treated mice, histopathological studies were carried out. Figure 3a depicts H&E staining of the tissues demonstrating the reduction of fatty infiltration in liver and Fig. 3b shows decreased macrophage infiltration
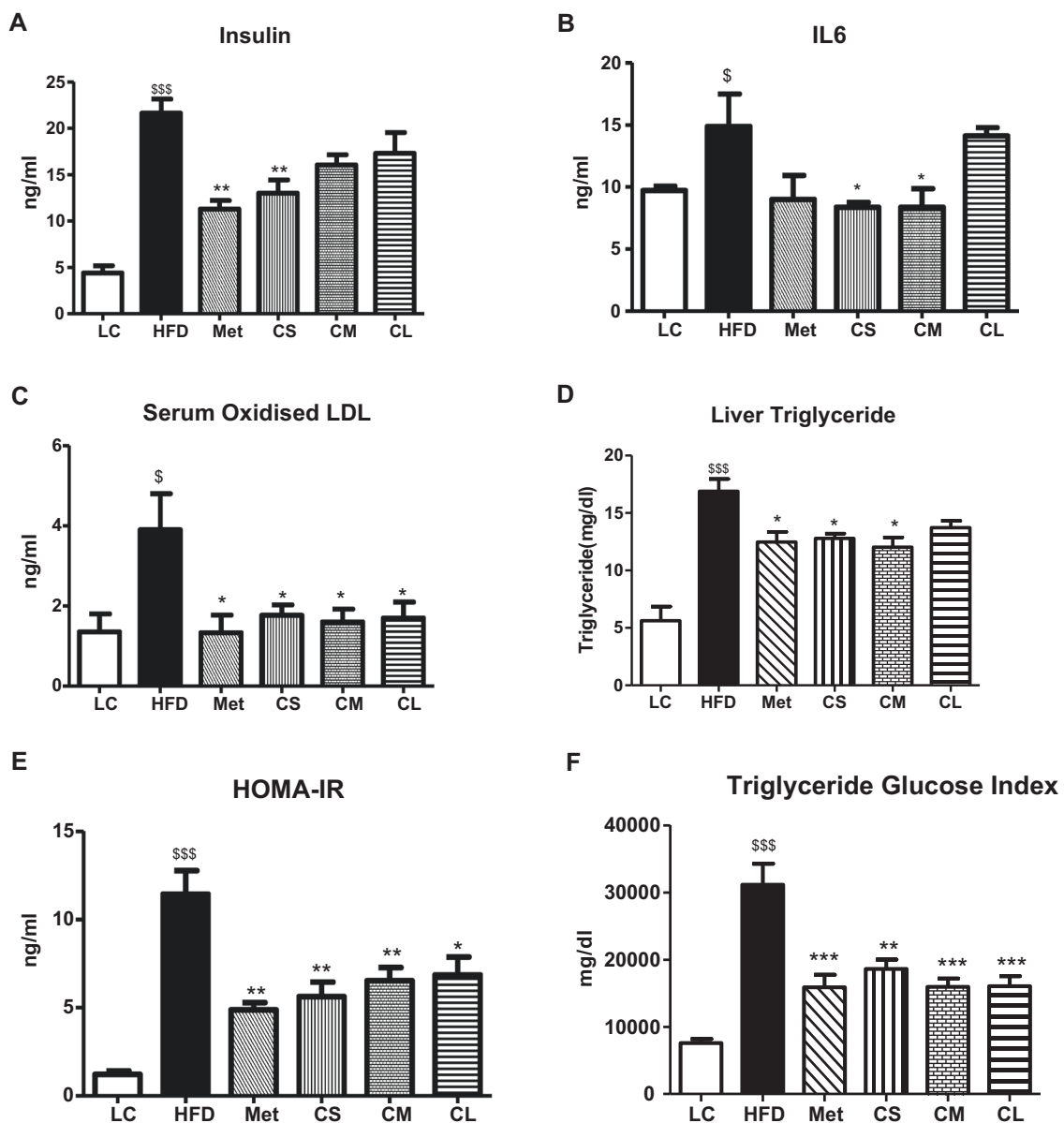
Fig. 2 Improvement in serum parameters and Insulin resistance measured at the time of termination: (**a**) Serum Insulin levels. (**b**) Serum IL6 levels. (**c**) Serum Oxidised LDL levels. (**d**) Liver Triglyceride Levels. (**e**) Measurement of IR using HOMA-IR. (**f**) Triglyceride glucose index

in adipose tissues mainly by CS at ×400 magnification. Figure 3c depicts reduced hypertrophy of the pancreatic islets by all the treatments at ×200 magnification.

Upregulation of miRNA-206 and increment in total protein content of the skeletal muscle
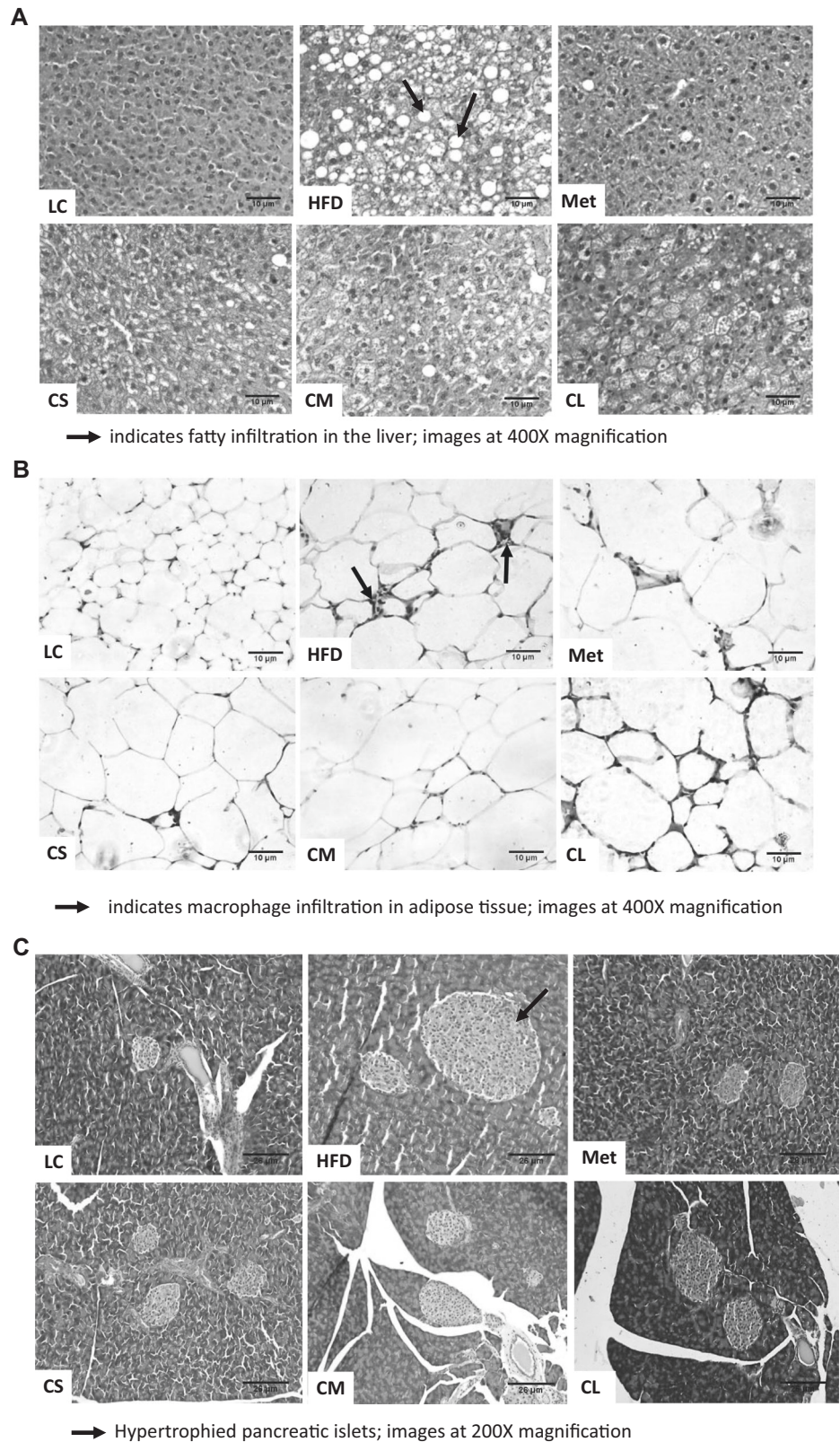
In an effort to investigate the role of miRNA-206 in DIO model and the effect of the treatments which can plausibly dictate the mechanism of actions of ADMSCs and the effect of *i.m.* injection we performed the gene expression studies of miRNA-206 in all the treatment groups. The
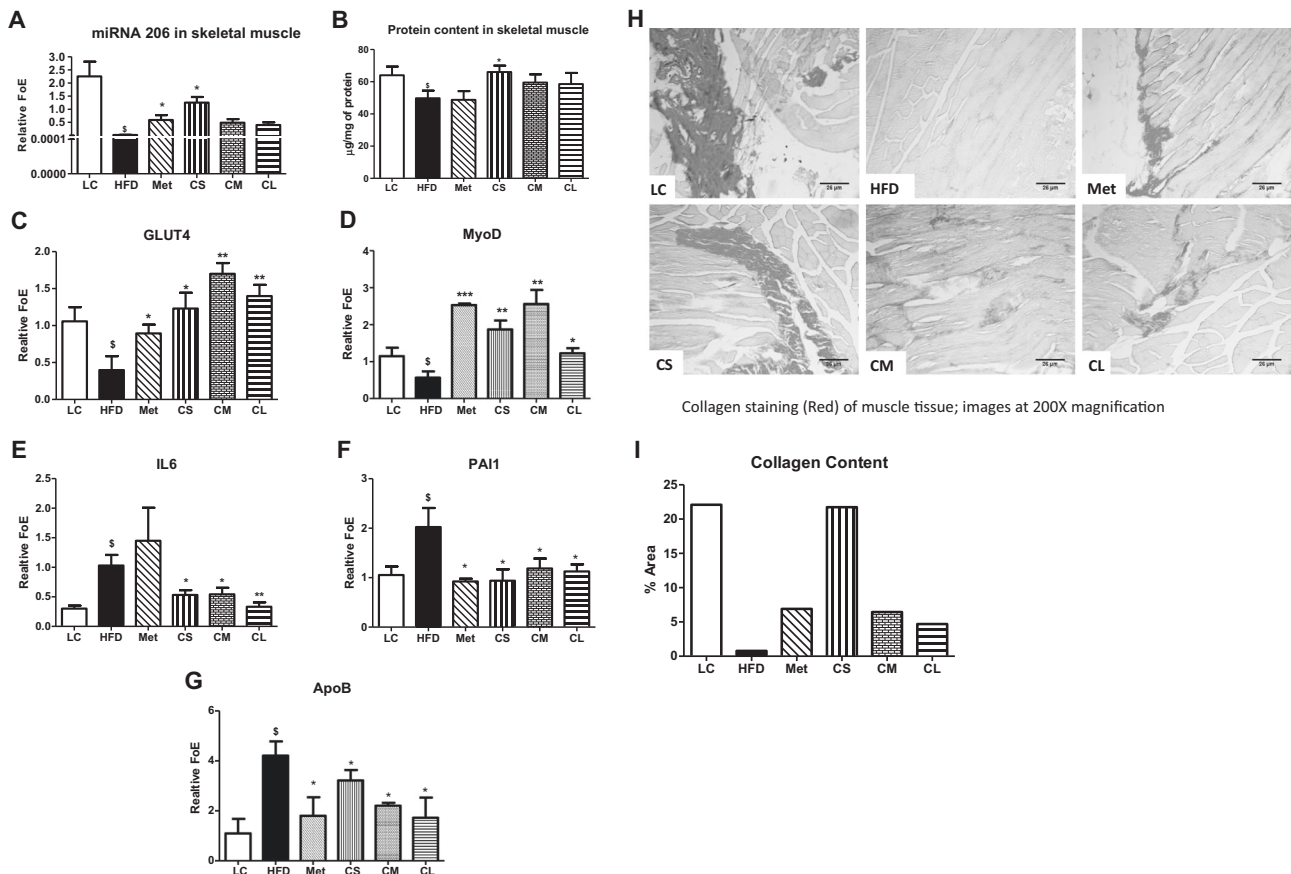
expression levels of miRNA-206 decreases remarkably in HFD fed mice and the levels of relative expression is brought up by CS treatment ($p < 0.05$) as shown in Fig. 4a. Figure 4b shows the dramatic increase in the protein content of the skeletal muscle only in the CS-treated group.

Improvement in gene expression pattern

Gene expression analysis was carried out for liver and muscle tissue samples. Figure 4c shows significant increase in the GLUT4 gene expression levels of the muscle tissue

Fig. 3 Representative images of histopathological examination different tissues after H&E staining: **a** Liver tissues showing recovery of the fatty infiltrated liver due to HFD.
b Subcutaneous adipose tissue sections depict the reduction of macrophage infiltration in the adipose tissue especially in the CS-treated group. **c** Hypertrophied islets in the pancreatic sections of untreated HFD control reduced in all the treatment groups. Liver and Subcutaneous adipose section images were captured at ×400 magnification and pancreas at ×200

→ indicates fatty infiltration in the liver; images at 400X magnification

→ indicates macrophage infiltration in adipose tissue; images at 400X magnification

→ Hypertrophied pancreatic islets; images at 200X magnification

Fig. 4 miRNA-206 expression level and protein content of the skeletal muscle: **a** miRNA-206 expression levels in skeletal muscle which was normalized to U6SnRNA gene. **b** Total protein content of the skeletal muscle. **c** GLUT4 gene expression in skeletal muscle. **d** MyoD in skeletal muscle. Expression levels of genes mediating inflammation in the liver *viz.* **e** IL6, **f** PAI1, and **g** ApoB. **h** Picrosirius red staining of muscle tissues showing collagen deposition. **i** Quantification of collagen stained sections. All data presented are mean ± SEM. Significance levels '$' shows HFD compared with LC and '*' shows comparison with untreated HFD control

indicating increase in the insulin sensitivity and an outstanding upregulation of MyoD gene (Fig. 4d) clearly defines the regeneration of muscle increasing the muscle mass through miRNA-206 as mentioned earlier. Gene expression analysis for the liver tissues showed remarkable decrease in IL6, PAI1, and ApoB depicted in Fig. 4e, f, g, respectively. Downregulation of these genes in all the treatments explain the reduction in the extent of inflammation in the liver.

Collagen deposition in muscle tissue

The increase in muscle mass led us to study the muscle structure. Picrosirius red staining of muscle tissue showed intense yellow myocyte staining and red collagen staining. The CS-treated group showed maximum collagen staining of all the treated groups in the muscle tissue. The images were captured using an inverted microscope (Nikon Eclipse TE2000–5, Japan) at ×200 magnification.

Cytokines detected in CM by LCMS/MS

Various beneficial cytokines were identified in the CM which is well known to improve the metabolic dysregulated conditions (Supplementary table)

Migration of labeled ADMSCs to different organs

The representative data in Fig. 5a show that after the intramuscular injection of the NIR-labeled ADMSCs exhibits NIR fluorescence that is focally localized parallel to the thigh at day 0 post transplantation. Normalized fluorescence (total relative fluorescence/total area) of the right and left thigh muscle is represented in Fig. 5b. The fluorescence in the right muscle is significantly higher on day 0 in comparison to week 4 and week 8. To confirm whether transplanted cells have migrated in different tissues, the organ imaging was performed at these same time points to confirm the biodistribution of these cells (Fig. 5c). The normalized signal intensity with respect to vehicle control is plotted in Fig. 5d.
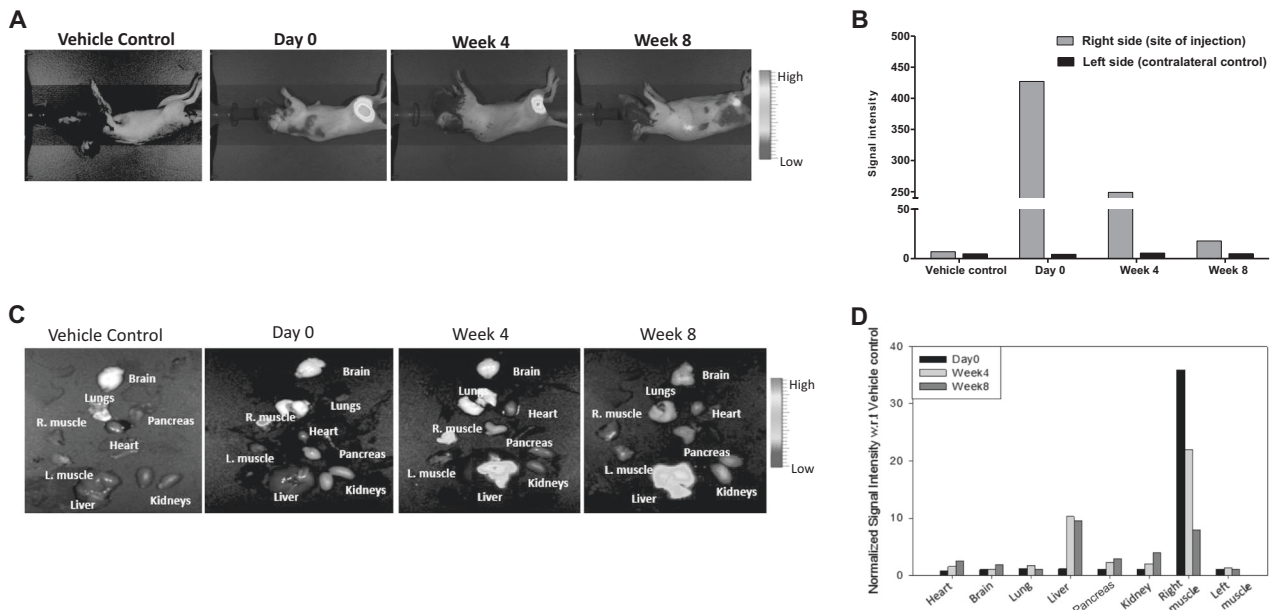
Fig. 5 Tracking the injected cells in vivo. **a** The heat map showing intramusclular injection of ADMSCs on the right muscle. **b** Normalized signal intensity. **c** The heat map showing the bio- distribution of cells in different organs at different day points. **d** Normalized signal intensity

Discussion

In the present investigation we compared the effect of human ADMSCs, their CM and their CL on metabolic dysregulation with respect to glycemic status, insulin resistance, triglycerides, proinflammatory cytokines viz. IL6, and Oxd LDL using metformin as a positive control. We found that amongst the three treatments-tested ADMSCs suspension (CS) was the best as it restored not only the organ function but also the tissue architecture as revealed by serum and histopathological analyses. Earlier reports showed the beneficial effect of MSC injection via *i.v.* route supporting our present study [6, 7]. However, this study is unique wherein we have shown the effect of human ADMSCs via *i.m.* route in ameliorating the ill effects of HFD. We chose *i.m.* route in order to facilitate slow release of their paracrine secretion into the systemic circulation. The logic behind using *i.m* route was a reported cross talk between skeletal muscle and pancreatic beta cell [16–18]. It is shown that a healthy muscle secretes myokines which positively impact the pancreatic beta cell, whereas a diabetic muscle secrete cytokines which negatively impacts the beta cell function. Moreover, in Indian population the muscle mass is always shown to be less than the fat mass as compared with the European community [19, 20]. Therefore we were interested in examining the effect of *i.m.* injections of ADMSCs on the metabolism of HFD fed mice.

The DIO model was developed following the similar procedure as reported earlier with slight modifications [13].

The establishment of DIO was confirmed by and substantial increase in body weight accompanied by hyperglycemia, hyperinsulinemia, hypertriglyceridemia, and abnormal OGTT. None of the treatments resulted in decrease in body weight as reported earlier with *i.v.* injection using rodent MSCs. The study by Cao et al. concluded that treatment with mouse ADMSCs was effective in lowering the blood glucose level and improving the glucose tolerance in mice along with decrease in body weight [6]. The striking feature of our study is the management of metabolic dysregulation caused by diet-induced obesity, which is the root cause of the metabolic syndrome [21–23]. As described earlier, in severe insulin resistance, there is a reduction in muscle GLUT4 protein and mRNA expression similar to adipose tissue [24]. The decrease in hyperglycemia and restoration of OGTT could be attributed to increased expression of GLUT4 in the skeletal muscle resulting in decreased IR and restoration of normoglycemia. HOMA-IR and TyG indicate a decrease in whole body insulin resistance in the treated group of mice. Altered gene expression has also been reported in non-alcoholic fatty liver disease [25–27]. The gene expression levels for IL6, PAI1 and ApoB in the liver were drastically reduced in all the treatment groups indicating the therapeutic value of ADMSCs and their by-product. It needs to be mentioned that metformin did not show any significant change in the level of IL6 gene expression suggesting its limitation.

All the treatment also led to decrease in pro inflammatory cytokine IL6 and lowering Oxd LDL except metformin and

CL which did not show any significant change in the reduction of secreted IL6. This was further confirmed by histological examinations of subcutaneous fat, liver, and pancreas. Subcutaneous fat exhibited decrease in macrophage infiltration indicating reduction in inflammation. It is known that HFD is one of the causes of fatty liver. NAFLD being one of the most common disease across the world. Rats fed with HFD develop IR, hypertriglyceridemia, hepatic steatosis, and liver damage, which is the characteristics of NAFLD [28, 29]. The treatment with CS as well as CM improved the fatty infiltration in the liver which was comparable to that of metformin-treated mice liver. Hypertrophy of the beta cell is the normal physiological response of the body to counteract obesity-induced IR [30]. Hypertrophy of the islets was observed in HFD mice pancreas which was found to be reduced in CS-treated mice.

With diet-induced obesity, metabolic dysfunction and the incidence of chronic low level inflammation can weaken the normal inflammatory response and the regenerative abilities of skeletal muscles, resulting in a pseudo-injury [31]. Association of type 2 diabetes with excessive loss of skeletal muscle and trunk fat mass in older adults is established [32]. Diabetes is widely known to be a muscle wasting disease. It has been reported that systemically administered MSCs could prevent muscle wasting associated with HFT-induced obesity and diabetes [33].

miRNAs have emerged lately and are known to be involved in many vital biological processes [34, 35]. There are reports stating that miRNA-206 expression is elevated in regenerated muscles [36]. We were interested in finding out the expression levels of miRNA-206 in skeletal muscle. We demonstrate for the first time a remarkable decrease in miRNA-206 expression of HFD mice as compared with that of lean control which was significantly upregulated in the CS- treated mice. We also found that HFT decreased the protein content of the muscle which was restored by CS-treated mice.

Based on our results we presumed that increase in fat mass decreases muscle mass and enhances metabolic dysfunction, which could be alleviated by *i.m.* injections of ADMSCs. Our results support this notion as evidenced by decrease in protein content and MyoD levels of the HFD mice skeletal muscle as compared with the lean control. On the contrary, the HFD mice injected with CS exhibited higher protein content demonstrating higher muscle mass and all treatment (CS, CM, and CL) showed significant upregulation of MyoD indicating regeneration of the muscle. Ma et al. reported that MiR-206 inhibits the expression of Pax7 and promotes the function of MyoD, thus establishing a positive regulatory feedback loop. Upregulation of miRNA-206 by MyoD further suppresses Pax7, thereby promoting muscle cell differentiation [37, 38]. Muscle

structure and function was restored by ADMSCs treatment as shown in the collagen deposition staining (Fig. 4h, i).

As stated by Gao et al., adipose tissue can produce extracellular vesicles from adipocytes as well as ADMSCs [39]. In the present study, LCMS/MS data demonstrates that CM contains most of the secreted cytokines and growth factors required for the betterment of dysregulated tissue. However, limited amount of factors exhaust soon after being used up by the damaged tissue and hence repeated injection of CM is required for a longer period of time for better results. On the contrary, CS injection shows the bio-distribution in different organs as demonstrated by in vivo tracking of cells. Our cell tracking data, clearly suggests that the bio-distribution of the transplanted ADMSCs occurs preferentially in liver by week 4 with trace signals measured from heart and kidney too and by week 8 it is distributed further in the brain and pancreas too.

Although daily oral treatment with metformin was found to be effective in decreasing IR, there are adverse effects associated with the long term treatment. CS has surpassed the role of metformin signifying its dominant role only with two injections showing organ specific effect. There are recent reports demonstrating the beneficial effect of ADMSCs treatment in obesity and diabetes [40–43]. Moreover, our data indicate for the first time the importance of intramuscular injection ADMSCs therapy in correcting obesity-induced metabolic dysregulation in DIO mice suggesting its possible therapeutic usage in human subjects.

Compliance with ethical standards

Conflict of interest The authors declare that they have no conflict of interest.

Publisher's note: Springer Nature remains neutral with regard to jurisdictional claims in published maps and institutional affiliations.

References

1. Hursting SD, Dunlap SM. Obesity, metabolic dysregulation, and cancer: a growing concern and an inflammatory (and micro-environmental) issue. Ann N Y Acad Sci. 2012;1271:82–7.
2. Collins KH, Herzog W, MacDonald GZ, Reimer RA, Rios JL, Smith IC, et al. Obesity, metabolic syndrome, and musculoskeletal

disease: common inflammatory pathways suggest a central role for loss of muscle integrity. Front Physiol. 2018;23:112.

3. Ranganath SH, Levy O, Inamdar MS, Karp JM. Harnessing the mesenchymal stem cell secretome for the treatment of cardiovascular disease. Cell Stem Cell. 2012;10:244–58.

4. Semedo P, Burgos-Silva M, Donizetti-Oliveira C, Saraiva Camara NO. How do mesenchymal stem cells repair? Stem Cells in Clinic and Research; 2011.

5. Pileggi A. Mesenchymal stem cells for the treatment of diabetes. Diabetes. 2012;61:1355–56.

6. Cao M, Pan Q, Dong H, Yuan X, Li Y, Sun Z, et al. Adipose-derived mesenchymal stem cells improve glucose homeostasis in high-fat diet-induced obese mice. Stem Cell Research & Therapy. 2015;6:208.

7. Badimon L, Onate B, Vilahur G. Adipose-derived mesenchymal stem cells and their reparative potential in ischemic heart disease. Rev Esp Cardiol. 2015;68:599–611.

8. Si Y, Zhao Y, Hao H, Liu J, Guo Y, et al. Infusion of mesenchymal stem cells ameliorates hyperglycemia in type 2 diabetic rats: identification of a novel role in improving insulin sensitivity. Diabetes. 2012;61:1616–25.

9. Ji AT, Chang YC, Fu YJ, Lee OK, Ho JK. Niche-dependent regulations of metabolic balance in high-fat-diet-induced diabetic mice by mesenchymal stromal cells. Diabetes. 2015;64:926–36.

10. Bueno Pde G, Yochite JN, Derigge-Pisani GF, Malmegrim de Farias KC, de Avó LR, Voltarelli JC, et al. Metabolic and pancreatic effects of bone marrow mesenchymal stem cells transplantation in mice fed high-fat diet. PLoS ONE. 2015;10:e0124369.

11. Shree N, Venkategowda S, Venkatranganna MV, Bhonde RR. Treatment with adipose derived mesenchymal stem cells and their conditioned media reverse carrageenan induced paw oedema in db/db mice. Biomed Pharmacother. 2017;90:350–3.

12. Shree N, Bhonde RR. Conditioned media from adipose tissue derived mesenchymal stem cells reverse insulin resistance in cellular models. J Cell Biochem. 2017;118:2037–43.

13. Wang CY, Liao JK. A mouse model of diet-induced obesity and insulin resistance. Methods Mol Biol. 2012;821:421–33.

14. Anil TM, Harish C, Lakshmi MN, Harsha K, Onkaramurthy M, Sathish Kumar V, et al. CNX-012-570, a direct AMPK activator provides strong glycemic and lipid control along with significant reduction in body weight; studies from both diet-induced obese mice and db/db mice models. Cardiovasc Diabetol. 2014;13:27.

15. Kilkenny C, Browne WJ, Cuthill IC, Emerson M, Altman DG. Improving bioscience research reporting: the ARRIVE guidelines for reporting animal research. PLoS Biol. 2010;8:e1000412.

16. Ayala JE, Samuel VT, Morton GJ, Obici S, Croniger CM, Shulman GI, et al. Standard operating procedures for describing and performing metabolic tests of glucose homeostasis in mice. Dis Model Mech. 2010;3:525–34.

17. Gopurappilly R, Bhonde R. Can multiple intramuscular injections of mesenchymal stromal cells overcome insulin resistance offering an alternative mode of cell therapy for type 2 diabetes? Med Hypotheses. 2012;78:393–5.

18. Bouzakri K, Plomgaard P, Berney T, Donath MY, Pedersen BK, Halban PA. Bimodal effect on pancreatic β-cells of secretory products from normal or insulin-resistant human skeletal muscle. Diabetes. 2012;60:1111–21.

19. Pedersen L, Hojman P. Muscle-to-organ cross talk mediated by myokines. Adipocyte. 2012;1:164–7.

20. Yajnik CS, Yudkin JS. The Y-Y paradox. Lancet. 2004;363:163.

21. Hardikar AA, Satoor SN, Karandikar MS, Joglekar MV, Puranik AS, Wong W, et al. Multigenerational undernutrition increases susceptibility to obesity and diabetes that is not reversed after dietary recuperation. Cell Metab. 2015;22:312–9.

22. Roberts CK, Hevener AL, Barnard RJ. Metabolic syndrome and insulin resistance: underlying causes and modification by exercise. Training. Compr Physiol. 2013;3:1–58.

23. Wannamethee SG, Lowe GD, Shaper AG, Rumley A, Lennon L, Whincup PH. The metabolic syndrome and insulin resistance: relationship to haemostatic and inflammatory markers in older non-diabetic men. Atherosclerosis. 2005;181:101–8.

24. Atkinson BJ, Griesel BA, King CD, Josey MA, Olson AL. Moderate GLUT4 overexpression improves insulin sensitivity and fasting triglyceridemia in high-fat diet-fed transgenic mice. Diabetes. 2013;62:2249–58.

25. Auguet T, Berlanga A, Guiu-Jurado E, Martinez S, Porras JA, Aragonès G, et al. Altered fatty acid metabolism-related gene expression in liver from morbidly obese women with non-alcoholic fatty liver disease. Int J Mol Sci. 2014;15:22173–87.

26. Targher G, Bertolini L, Scala L, Zenari L, Lippi G, Franchini M, et al. Plasma PAI-1 levels are increased in patients with non-alcoholic steatohepatitis. Diabetes Care. 2007;30:e31–2.

27. Moon BC, Hernandez-Ono A, Stiles B, Wu H, Ginsberg HN. Apolipoprotein B secretion is regulated by hepatic triglyceride, and not insulin, in a model of increased hepatic insulin signaling. Arterioscler Thromb Vasc Biol. 2012;32:236–46.

28. Bravo E, Palleschi S, Aspichueta P, Buqué X, Rossi B, Cano A, et al. High fat diet-induced non alcoholic fatty liver disease in rats is associated with hyperhomocysteinemia caused by down regulation of the transsulphuration pathway. Lipids Health Dis. 2011;10:60.

29. Ferolla SM, Silva L, Ferrari Mde L, da Cunha AS, Martins Fdos S, Couto CA, et al. Dietary approach in the treatment of non-alcoholic fatty liver disease. World J Hepatol. 2015;7:2522–34.

30. Roat R, Rao V, Doliba NM, Matschinsky FM, Tobias JW, Garcia E, et al. Alterations of pancreatic islet structure, metabolism and gene expression in diet-induced obese C57BL/6J mice. PLoS ONE. 2014;9:e86815.

31. Collins KH, Hart DA, Reimer RA, Seerattan RA, Banker CW, Sibole SC, et al. High-fat high-sucrose diet leads to dynamic structural and inflammatory alterations in the rat vastus lateralis muscle. J Orthop Res. 2016;34:2069–78.

32. Park SW, Goodpaster BH, Lee JS, Kuller LH, Boudreau R, de Rekeneire N, et al. Excessive loss of skeletal muscle mass in older adults with type 2 diabetes. Diabetes Care. 2009;32:1993–7.

33. Abrigo J, Rivera JC, Aravena J, Cabrera D, Simon F, Ezquer F, et al. High fat diet-induced skeletal muscle wasting is decreased by mesenchymal stem cells administration: implications on oxidative stress, ubiquitin proteasome pathway activation, and myonuclear apoptosis. Oxid Med Cell Longev. 2016;2016:9047821.

34. Pillai RS. MicroRNA function: multiple mechanisms for a tiny RNA? RNA. 2005;11:1753–61.

35. Tranzer A, Stadler PF. Evolution of microRNAs. Methods Mol Biol. 2006;342:335–50.

36. Liu N, Williams AH, Maxeiner JM, Bezprozvannaya S, Shelton JM, Richardson JA, et al. microRNA-206 promotes skeletal muscle regeneration and delays progression of Duchenne muscular dystrophy in mice. J Clin Investig. 2012;122:2054–65.

37. Ma Guoda, Wang Yajun, Li You, Cui Lili, Zhao Yujuan, Zhao Bin, et al. MiR-206, a key modulator of skeletal muscle development and disease. Int J Biol Sci. 2015;11:345–52.

38. Dey BK, Gagan J, Dutta A. miR-206 and -486 induce myoblast differentiation by downregulating Pax7. Mol Cell Biol. 2011;31:203–14.

39. Gao X, Salomon C, Freeman DJ. Extracellular vesicles from adipose tissue—a potential role in obesity and type 2 diabetes? Front Endocrinol. 2017;8:202.

40. Vyas B, Shah A, Marathe A, Ansarullah, Vyas R, Bhonde R. Adipose tissue: a natural resource for multipotent mesenchymal

stem cells with potential translation to trigerminal layers. Indian J Plast Surg. 2018;51:177–81.

41. Ejarque M, Ceperuelo-Mallafré V, Serena C, Maymo-Masip E, Duran X, Díaz-Ramos A et al. Adipose tissue mitochondrial dysfunction in human obesity is linked to a specific DNA methylation signature in adipose-derived stem cells. Int J Obes. 2018; https://doi.org/10.1038/s41366-018-0219-6.

42. Payab M, Goodarzi P, Heravani NF, Hadavandkhani M, Zarei Z, Falahzadeh K, et al. Stem cell and obesity: current state and future perspective. Adv Exp Med Biol. 2018;1089:1–22.

43. Goodarzi P, Alavi-Moghadam S, Sarvari M, Tayanloo Beik A, Falahzadeh K, Aghayan H, et al. Adipose tissue-derived stromal cells for wound healing. Adv Exp Med Biol. 2018;1089:1–22.